Structures and biological activity of phosphorylated dihydroceramides of *Porphyromonas gingivalis*

Frank C. Nichols,[1,*] Birgit Riep,[*,†] JiYoung Mun,[§] Martha D. Morton,[§] Mike T. Bojarski,[*] Floyd E. Dewhirst,[**] and Michael B. Smith[§]

Department of Periodontology,* University of Connecticut School of Dental Medicine, 263 Farmington Avenue, Farmington, CT; Department of Periodontology and Synoptic Dentistry,† Charité University of Medicine Berlin, Augustenburger Platz 1, Berlin, Germany; Department of Chemistry,§ U3060 University of Connecticut, 55 North Eagleville Road, Storrs, CT; and Department of Molecular Genetics,** Forsyth Institute, 140 The Fenway, Boston, MA

Abstract ***Porphyromonas gingivalis*, a recognized periodontal pathogen, synthesizes free ceramides as well as other phosphorylated ceramide lipids. The purpose of this study was to separate complex lipids of *P. gingivalis* by high-performance liquid chromatography (HPLC) and determine the structures and biological activities of the major ceramide classes. Using gas chromatography-mass spectrometry, electrospray tandem mass spectrometry (ESI-MS/MS) and NMR analyses, three major classes of dihydroceramides were identified in specific HPLC fractions, with all classes containing the same dihydroceramide base structures (3-OH *iso*$C_{17:0}$ in amide linkage to saturated long-chain bases of 17, 18, or 19 carbons). The free dihydroceramide class recovered in HPLC fractions 7–8 revealed little biological activity. HPLC fraction 20 dihydroceramides, substituted with 1-*O*-phosphoglycerol and *iso*$C_{15:0}$ linked to the hydroxyl of 3-OH *iso*$C_{17:0}$, significantly potentiated interleukin-1β (IL-1β)-mediated prostaglandin secretion and produced marked alterations in fibroblast morphology. HPLC fraction 28 dihydroceramides, substituted with 1-*O*-phosphoethanolamine, demonstrated little capacity to potentiate IL-1β-mediated prostaglandin secretion. The novel phosphorylated dihydroceramides synthesized by *P. gingivalis* demonstrate varying biological activities based on the phosphorylated head group substitution and/or the addition of esterified fatty acid. These results also demonstrate the strong virulence capacity of phosphoglycerol dihydroceramides of *P. gingivalis* to promote inflammatory factor secretion from IL-1β-treated fibroblasts and to produce marked alterations in cell morphology in culture.**—Nichols, F. C., B. Riep, J. Mun, M. D. Morton, M. T. Bojarski, F. E. Dewhirst, and M. B. Smith. **Structures and biological activity of phosphorylated dihydroceramides of *Porphyromonas gingivalis*. *J. Lipid Res.* 2004.** 45: **2317–2330.**

Supplementary key words phosphoethanolamine ceramide • phosphoglycerol dihydroceramide • interleukin-1β • prostaglandin E_2 • gingival fibroblast • long-chain base • gas chromatography-mass spectrometry • electrospray MS/MS

Inflammatory periodontal disease in adults is initiated with the accumulation of specific bacteria in the sulcus around the teeth followed by a chronic inflammatory reaction to these organisms by the host. The anaerobic, Gram-negative organism, *Porphyromonas gingivalis*, is thought to be a major periodontal pathogen (1) associated with inflammatory periodontal disease in adults. Dihydroceramide lipids of *P. gingivalis* and other phylogenetically related organisms have been identified in lipid extracts of diseased tooth roots and diseased gingival tissues (2). Lipid extract of *P. gingivalis* is known to potentiate prostaglandin secretion from gingival fibroblasts when cotreated with interleukin-1β (IL-1β) (3). However, little is known about the specific lipids responsible for this biological activity. Therefore, the primary goal of this study was to determine whether the dominant dihydroceramide lipids of *P. gingivalis* contribute to the observed biological activity. To clarify this question, the dihydroceramide lipids of *P. gingivalis* were first separated into constituent fractions before structural analysis and biological testing. The biological activities of *P. gingivalis* dihydroceramides are important to assess, given the recent evidence that other microbes synthesize ceramide lipids that induce apoptosis (4).

As originally described for *Bacteroides fragilis* (5), *P. gingivalis* synthesizes free dihydroceramides containing 3-hydroxy *isobranched (iso)* $C_{17:0}$ linked to either an 18- or 19-carbon saturated long-chain base (2). On the basis of gas liquid chromatography-mass spectrometry (GC-MS) analysis of *P. gingivalis* lipid extracts, two additional free

Manuscript received 20 July 2004 and in revised form 21 September 2004.

Published, JLR Papers in Press, October 1, 2004.
DOI 10.1194/jlr.M400278-JLR200

[1]To whom correspondence should be addressed.
e-mail: nichols@nso.uchc.edu

dihydroceramides of *P. gingivalis* were proposed to contain $C_{17:1}$ (α-β unsaturated) linked to the long-chain bases listed above. Although $C_{17:1}$ is recovered in *P. gingivalis*, catalytic hydrogenation did not increase the mass of these ceramides. Therefore, specific structural characteristics of these dihydroceramides were not confirmed (2). Given in this report is evidence, provided by separating the lipids of *P. gingivalis* into component fractions and analyzing the lipids using additional analytical techniques, that clarifies the structures of the proposed unsaturated ceramides.

MATERIALS AND METHODS

P. gingivalis (ATCC 33277, type strain) was inoculated into cooked meat medium supplemented with trypticase, yeast extract, menadione, and hemin (BBL, #295982, Becton Dickinson, Franklin Lakes, NJ). Once growth was established, the initial culture was inoculated into enriched thioglycollate medium (BBL) and prereduced blood agar plates. Batch suspension cultures were established after verification of anaerobic growth of Gram-negative rods in thioglycollate medium and demonstration of black-pigmented bacterial colonies on blood agar plates under anaerobic culture conditions. Batch suspension cultures (1 l flasks) were grown in basal [peptone, trypticase, and yeast extract, (BBL)] medium supplemented with hemin and menadione (Sigma; St. Louis, MO) and brain heart infusion. The suspension cultures were incubated in an anaerobic chamber flushed with N_2 (80%), CO_2 (10%), and H_2 (10%) at 37°C for five days, and the bacteria were harvested by centrifugation (3,000 *g* for 20 min). Following lyophilization, ~4 g of *P. gingivalis* pellet was extracted overnight using a modification of the phospholipid extraction procedures of Bligh and Dyer (6) and Garbus et al. (7). Specifically, 4 ml of H_20 + 16 ml of MeOH-$CHCl_3$ (2:1; v/v) was added to the bacterial sample and vortexed. After 12 h, 3 ml of 2 N KCl + 0.5 M K_2HPO_4 and 3 ml $CHCl_3$ were added and the sample vortexed. The lower organic phase was carefully removed and $CHCl_3$ (3 ml) was added to each sample and vortexed. The $CHCl_3$ phase was removed and combined with the previous organic solvent extract. The lipid extract from *P. gingivalis* was dried under nitrogen and stored frozen.

Fractionation of bacterial lipids by high-performance liquid chromatography (HPLC) was accomplished using a semipreparative HPLC column (1 × 25 cm silica gel, 5 μm; Supelco, Inc., Bellefonte, PA) and eluted isocratically with hexane-isopropanol-water (6:8:0.75; v/v/v: solvent A) (8). Lipid samples were dissolved in solvent A to achieve a concentration of ~80 mg/ml. For each chromatographic separation, 3 mg of lipid was applied and fractions were pooled for 25 column fractionations. Samples were eluted at 2.0 ml/min with 1 min fractions collected. Fractions were dried under nitrogen and resuspended in 2 ml of $CHCl_3$. Lipid recovery in each HPLC fraction was determined by drying 5 μl from each fraction onto a microbalance tray and weighing the tray using a Cahn Electrobalance (Ventron Corporation, Cerritos, CA). An additional 10 μl from each fraction was analyzed for dihydroceramide constituents using GC-MS as described below. Fractions containing specific dihydroceramide lipids were pooled and repurified using the same column and elution conditions. The repurified lipids were evaluated for dihydroceramide recovery using GC-MS.

Lipid film preparation

Predetermined amounts of enriched dihydroceramide lipid fractions were transferred in $CHCl_3$ to conical vials and dried. The selected HPLC fractions were then dissolved in ethanol to achieve a final concentration of 0.5 μg/μl, and 20 μl of each lipid fraction was deposited in 35 mm culture wells while the culture dishes were maintained in a laminar flow hood. The ethanol was allowed to evaporate overnight, leaving a lipid residue covering most of the culture well surface. Vehicle control wells received only ethanol solvent. Lipids were deposited onto culture dishes in this manner so that cells could be exposed to bacterial lipid fractions without introducing organic solvent into the culture medium.

Primary cultures of gingival fibroblasts were obtained using a single gingival tissue explant harvested at the time of periodontal surgery and processed as previously described (9). Gingival tissue samples were obtained according to a protocol approved by the University of Connecticut Health Center Institutional Review Board, and participants provided written informed consent. Primary cultures of gingival fibroblasts were grown in Minimal Essential Medium (MEM) supplemented with 10% fetal calf serum, penicillin G (100 U/ml), streptomycin (100 μg/ml), and amphotyricin B (0.25 μg/ml) (Sigma), and cells were passaged fewer than 10 times for these experiments. The cells were harvested using trypsin (0.1%, w/v) in Ca^{2+}-, Mg^{2+}-free phosphate-buffered saline and resuspended in MEM medium to achieve a 1:3 dilution of cells for passaging. Cells were cultured in an H_2O-saturated, 5% CO_2 atmosphere at 37°C. When fibroblasts were treated with bacterial lipids, cells were inoculated into culture wells to achieve a cell number/surface area equivalent to confluent cultures. After 2 h of exposure to bacterial lipids, the culture medium was supplemented with either control medium or medium containing recombinant human IL-1β (final concentration,10 ng/ml) (Immunex; Seattle, WA). The cultures were then incubated for an additional 24 h, after which the medium samples were harvested and frozen.

Quantification of prostaglandins in culture medium samples

Prostaglandin $F_{2\alpha}$ ($PGF_{2\alpha}$), 6-keto $PGF_{1\alpha}$, and prostaglandin E_2 (PGE_2) were quantified in medium samples using a modification of the method of Luderer et al. (10), previously described by Nichols (2). Each medium sample was supplemented with 100 ng of D_4-$PGF_{2\alpha}$, D_4-6-keto $PGF_{1\alpha}$, and D_4-PGE_2. The fibroblast medium samples were thawed and the pH adjusted to pH 3.5 with concentrated formic acid. The acidified medium samples were then applied to reverse-phase preparative columns [Supelclean, LC-18 SPE tubes, 6 ml; Supelco, Inc.] mounted on a vacuum manifold. Before applying the medium samples, the C-18 columns (3 ml) were regenerated by running sequentially 3 ml of 100% methanol followed by 3 ml of Ca^{2+}-Mg^{2+}-free phosphate-buffered saline (pH 3.5). Each acidified medium sample was then applied to individual SPE columns, the columns were washed with 3 ml of 25% methanol in water, and enriched prostaglandins were eluted with 3 ml of 100% methanol. The resultant samples were then supplemented with 2 ml of 1% formic acid in water, and the prostaglandins were extracted twice with 2 ml of chloroform. The chloroform extracts were dried under nitrogen.

All derivatizing agents were obtained from Pierce Chemical Corp. (Rockford, IL). Prostaglandin samples were derivatized using the method of Waddell, Blair, and Wellby (11). Prostaglandin samples were first treated with 2% methoxylamine hydrochloride in pyridine (30 μl). After standing overnight at room temperature, the samples were dried under nitrogen, dissolved in acetonitrile (30 μl), and treated with pentafluorobenzyl bromide (35% v/v in acetonitrile, 10 μl) and diisopropylethylamine (10 μl). The samples were vortexed, incubated for 20 min at 40°C, and evaporated under nitrogen. The residue was then treated

with bistrimethylsilyl-trifluoroacetamide (BSTFA, 50 μl) and allowed to stand at room temperature for 4–5 days.

Synthesis of isobranched long-chain bases

The *erythro* 17-methyl octadecasphinganine was synthesized according to the stereoselective synthesis of sphingosine developed by Nimkar, Menaldino, and Liotta (12). D-erythro-17-methyl octadecasphinganine was obtained by hydrogenation of the oxazolidine 1, prepared from Garner's aldehyde and 1-lithio-17-methyloctadec-1-yne, followed by deprotection with a mixture of trifluoroacetic acid and water in a ratio of 10:1 (76%, 3 steps). 17-Methyloctadec-1-yne was prepared in 3 steps from 10-bromo-1-decene and 1-bromo-4-methylbutane according to the synthesis of 12-methyltridec-1-yne developed by Mori and colleagues (63%, 3 steps) (13). The *erythro* 15-methyl hexadecasphinganine was synthesized using the same synthetic scheme.

Analysis of bacterial fatty acid, long-chain base, and dihydroceramide lipid components in HPLC fractions

Analysis of esterified fatty acids was accomplished by treating a sample of the lipid fraction with 0.5 N $NaOCH_3$ in anhydrous methanol (0.5 ml, 40°C for 20 min). The reaction was stopped with the addition of 100 μl of glacial acetic acid and 1 ml of water. The sample was then extracted twice with hexane and the contents dried under nitrogen. The sample was reconstituted in hexane for GC-MS analysis. For long-chain base and amide-linked fatty acid analyses, samples of HPLC fractions were hydrolyzed in 4 N KOH (0.5 ml, 100°C for 14 h). After cooling, the sample was extracted twice with 2 ml of $CHCl_3$ and dried under nitrogen. Trimethylsilyl (TMS) derivatives of long-chain bases were prepared by treating with BSTFA (40 μl, room temperature overnight). Synthetic standards of isobranched long-chain bases and dihydrosphingosine standard obtained from Matreya, Inc. (Pleasant Gap, PA) were treated to form TMS derivatives using the same method. For GC-MS analysis of dihydroceramide samples, selected HPLC fractions were treated with BSTFA (50 μl) and allowed to stand overnight at room temperature.

GC-MS analysis

Derivatized products of hydroxy fatty acids, long-chain bases, and prostaglandins were transferred to vials used for GC-MS automated sampling (crimp cap vials, 200 μl). GC-MS was carried out on a Hewlett Packard (Avondale, PA) 5890-gas chromatograph interfaced with a 5988A-mass spectrometer. Prostaglandin samples were applied to an SPB-1 (12 m × 0.2 mm, 0.33 μm film thickness; Supelco, Inc.) column held at 100°C. Prostanoid samples were analyzed using a temperature program of 5°C/min from 100°C to 240°C. The injector block was held at 260°C, and the transfer tube was maintained at 280°C. Prostaglandin levels were quantified using selected ion monitoring of the characteristic base peak ions, and bacterial fatty acids and long-chain bases were detected and interpreted through analysis of characteristic spectra.

TMS derivatives of bacterial fatty acids and long-chain bases were analyzed using gas chromatography combined with electron impact mass spectrometry. The sample was applied to an SPB-1 (12 m × 0.2 mm, 0.33 μm film thickness; Hewlett Packard) column held at 100°C. The fatty acid and long-chain base samples were injected using the splitless mode (30 s), and the column was heated at 10°C/min to 270°C. The injector block was held at 260°C, and the transfer tube was maintained at 280°C. The mass spectrometer was used with the ion source temperature at 150°C, the electron energy at 70 eV, and an emission current of ~300 mA. Total ion spectra were acquired using a range of *m/z* 50 to 800, and the spectra for individual peaks were evaluated for fatty acid and long-chain base products.

For dihydroceramide analyses, selected HPLC fractions were treated to form TMS derivatives and were applied to an SPB-1

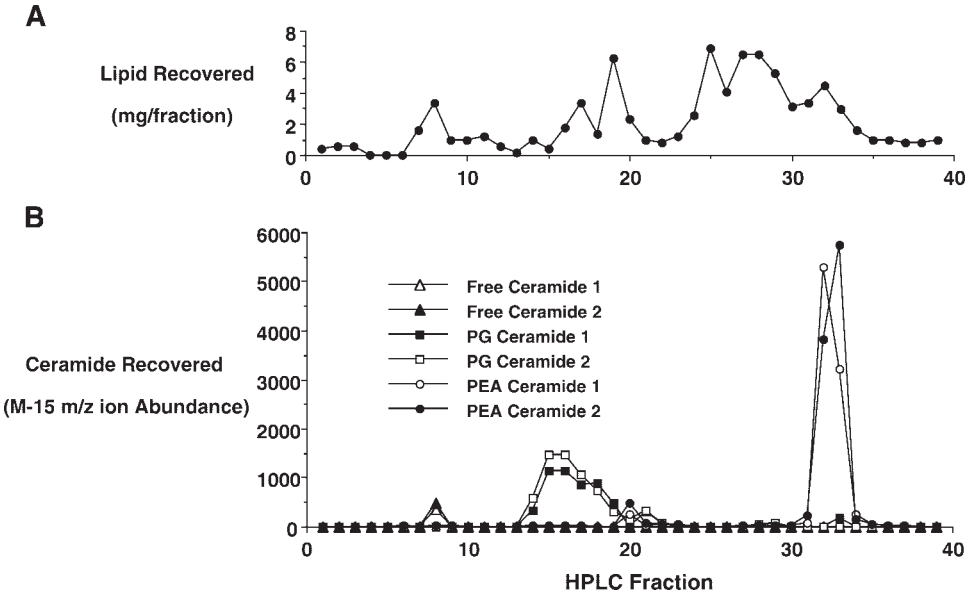

Fig. 1. High-performance liquid chromatography (HPLC) fractionation of *Porphyromonas gingivalis* lipids. Lipids of *P. gingivalis* were extracted and separated as described in Materials and Methods. A: Mass recovery of lipid in each fraction. B: Recovery of the three major ceramide classes using gas liquid chromatography-mass spectrometry (GC-MS) detection of the characteristic M-15 ions. The free dihydroceramides 1 and 2 recovered in HPLC fractions 7–8 were detected as 784 and 770 *m/z* ions, as previously described (2). The phosphoglycerol dihydroceramides 1 and 2 were detected using the M-15 ions depicted in Fig. 6. The phosphoethanolamine dihydroceramides 1 and 2 were detected using M-15 ions depicted in Fig. 7. The recovery of lipid in each fraction is shown for a total of 39 fractions.

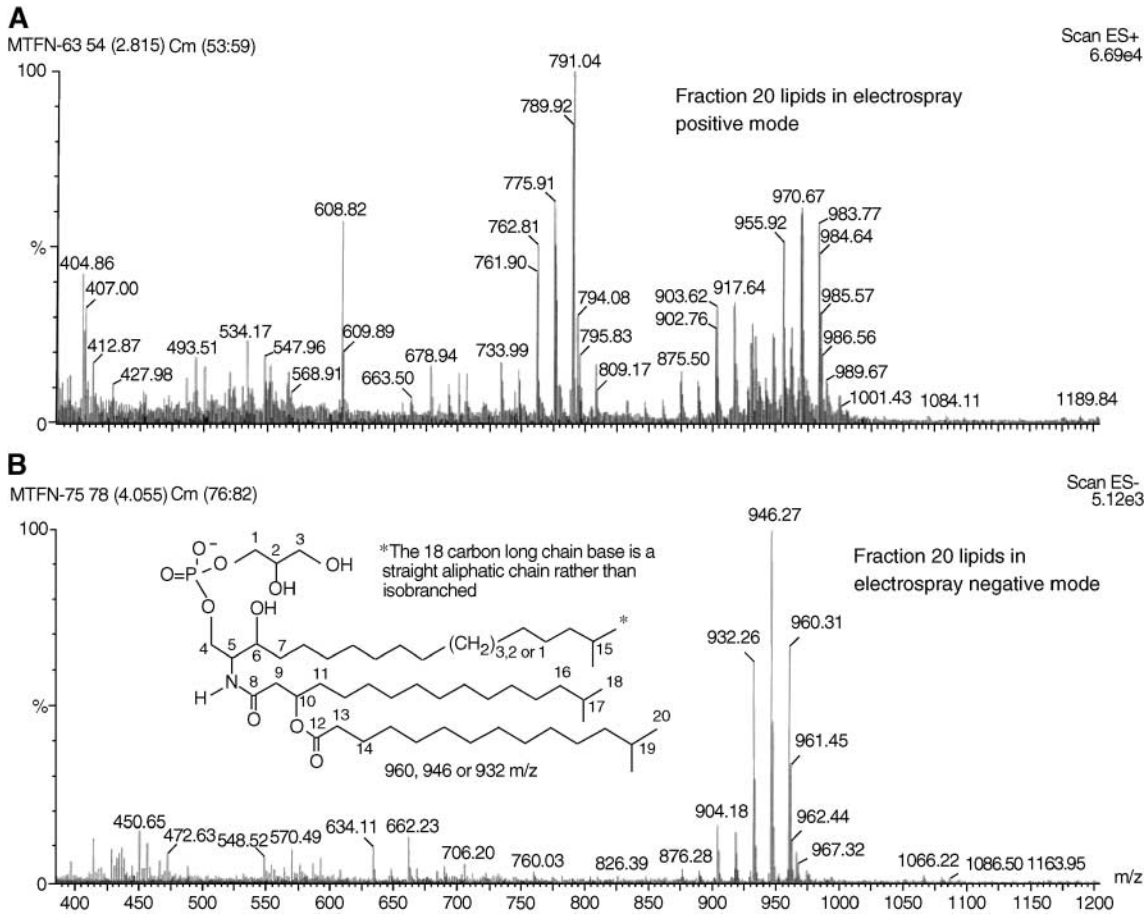

Fig. 2. Positive and negative electrospray-mass spectrometry (ESI-MS) of HPLC fraction 20 lipids. See the Materials and Methods section for the details of the ESI-MS analyses. The ESI (+) (A) and (−) (B) mass spectra for fraction 20 lipids. The proposed phosphoceramide structures are numbered for reference to the NMR carbon and proton spin assignments (shown in Table 1). Details of the structural reconciliation are included in Figs. 2–6 and are reviewed in the Results and Discussion sections.

column (15 m × 0.25 mm, 0.1 μm film thickness; Supelco, Inc., Bellefonte, PA). Complex lipid samples were injected with the inlet block at 310°C using the splitless mode with a temperature program of 10°C/min from 200°C to 300°C followed by 5°C/min to 310°C and 4 min at 310°C. The mass spectrometer was used in the electron impact ionization mode with the ion source temperature at 150°C, an electron energy of 70 eV, and an emission current of ~300 mA. The injector block and transfer tube were held

TABLE 1. NMR spectral analysis of HPLC fraction 20 lipids

^{1}H	^{13}C HMQC	^{13}C HMBC	TOCSY
[10] 5.22 (m, 1H)	70.6	*[12]* 173.9, *[8]* 170.5, 40.7, 33.6	2.50, 1.60
[4] 4.20 (m, 1H-^{31}P)	64.2		3.85, 3.63, 1.60, 1.35
[1] 3.88 (m, 2H-^{31}P)	66.4	71.1, 62.1	3.75, 3.60, 3.58
[4] 3.85 (1H, J = 22.4 H)	64.2		
[5] 3.80 (m, 1H)	54.7		
[2] 3.75 (m, 1H)	71.1		
[6] 3.63 (m, 1H)	69.4		
[3] 3.60 (dd, 1H, J = 5.7, 8.1)	62.4		
[3] 3.58 (dd, 1H, J = 5.7,8.1)	62.4		
[9] 2.50 (d, 2H, J = 6.2)	40.7	70.6, 33.6	5.27, 1.61
[13] 2.31 (d, 2H, J = 7.2	34.4	28.8	24.7
[7,11,14] 1.60 (bs)	33.7, 25.8		
[15,17,19] 1.51 (m, 4H)		22.2, 38.8	
1.27 (bs, 53H)	30.8–28.0	38.8, 29.3, 27.1	
[17] 1.16 (m, 1H)	38.8	29.3, 27.1, 22.2	
[18, 20] 0.86 (d, 12H, J = 6.4)	22.2	22.2, 27.7, 38.8	
[16] 0.85 (t, 3H)	13.4		

The numbers in italicized brackets correspond to the numbers on the chemical structure depicted in Fig. 2. HPLC, high-performance liquid chromatography.

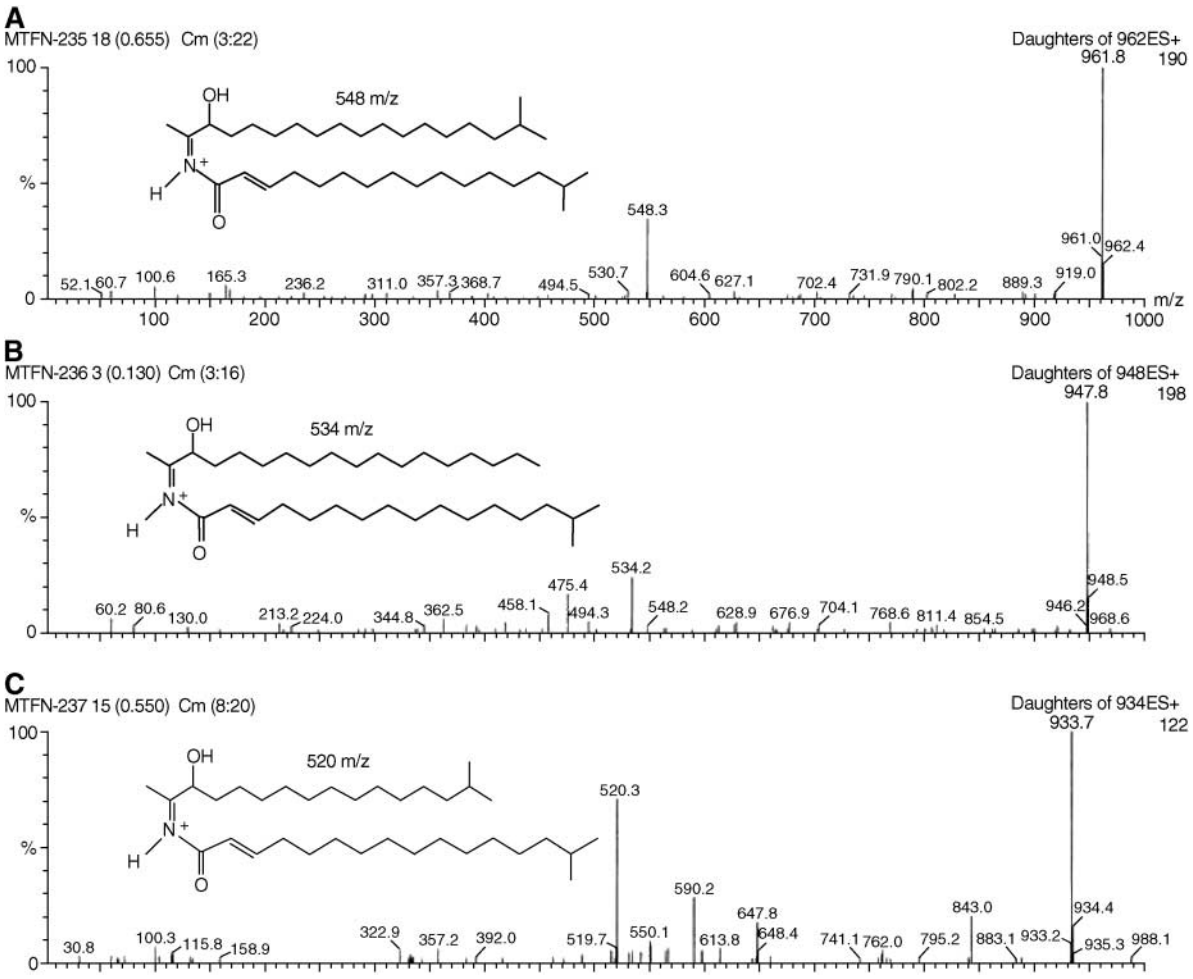

Fig. 3. ESI (+) MS/MS of the 962, 948, and 934 *m/z* parent phosphorylated dihydroceramides of *P. gingivalis*. The ESI (+) MS/MS analysis is described in the Materials and Methods section. Frames A, B, and C represent the parent daughter spectra for the 962, 948, and 934 *m/z* parent phosphoceramides, respectively. The daughter ions (548, 534, and 520 *m/z*) are indicated by the associated chemical structures.

at 310°C. For positive-ion chemical ionization analyses, methane was used as the reagent gas and was maintained at 0.5 torr and the ion source temperature was held at 150°C.

Electrospray tandem mass spectrometry analysis of dihydroceramide lipids

Electrospray tandem mass spectrometry (ESI-MS/MS) analysis was accomplished using a Micromass Quattro II mass spectrometer system. Dihydroceramide lipid fractions were dissolved in hexane-isopropanol (6:8, v/v, elution solvent), and the samples were injected at a maximum concentration of 100 μg/ml. Lipid samples (10 μl) were infused at a flow rate of 20 μl/min. For electrospray positive-ion analyses, the desolvation and inlet block temperatures were 100°C and 150°C, respectively, and the transcapillary potential was 3,500 volts. For electrospray negative-ion analyses, the desolvation and inlet block temperatures were 80°C and 100°C, respectively, and the transcapillary potential was 3,000 volts. The cone voltage was usually 30 volts, and the mass acquisition range was 0–2,000 amu for initial electrospray MS analyses. MS/MS analysis used a collision energy of between 28 and 30 volts, and argon was introduced at a pressure of 10^{-2} to 10^{-4} torr. The gas and collision energies were adjusted to minimize parent ion recoveries and maximize daughter ion recoveries. These conditions were used for both positive- and negative-ion ESI-MS/MS analyses.

NMR analyses

NMR data were collected on a Bruker (Rheinstetten, Germany) DRX-400, a Bruker Avance 500, and a Varian (Palo Alto, CA) INOVA 600 (operating frequencies 400.144 MHz, 500.13 MHz, and 599.75 MHz, respectively). One-dimensional ^{1}H, ^{13}C, and ^{31}P, as well as two-dimensional ^{1}H-^{1}H (COSY), ^{1}H-^{13}C (g-HMQC), ^{1}H-C-C-^{13}C (g-HMBC), TOCSY, NOESY, and ^{1}H-^{31}P (gHMBC) were acquired for HPLC fraction 20 lipids dissolved in a mixture of deuterated solvents ($CDCl_3$-CD_3OD). These data allowed the assignment of proton and carbon resonances of the dihydroceramide base and the phosphate side-chain of the molecule, as well as specific components of the aliphatic chains. A mixture of solvents was necessary in order to prevent aggregation into micelles or reverse micelles, depending on the solvent.

Data analysis

Statistical tests included one-factor ANOVA comparing prostaglandin secretion between culture treatment groups and the Fisher PLSD or Scheffe F-tests for significant differences between treatment categories.

RESULTS

Lipids were extracted from *P. gingivalis* and separated by HPLC as shown in **Fig. 1**. GC-MS analysis revealed three

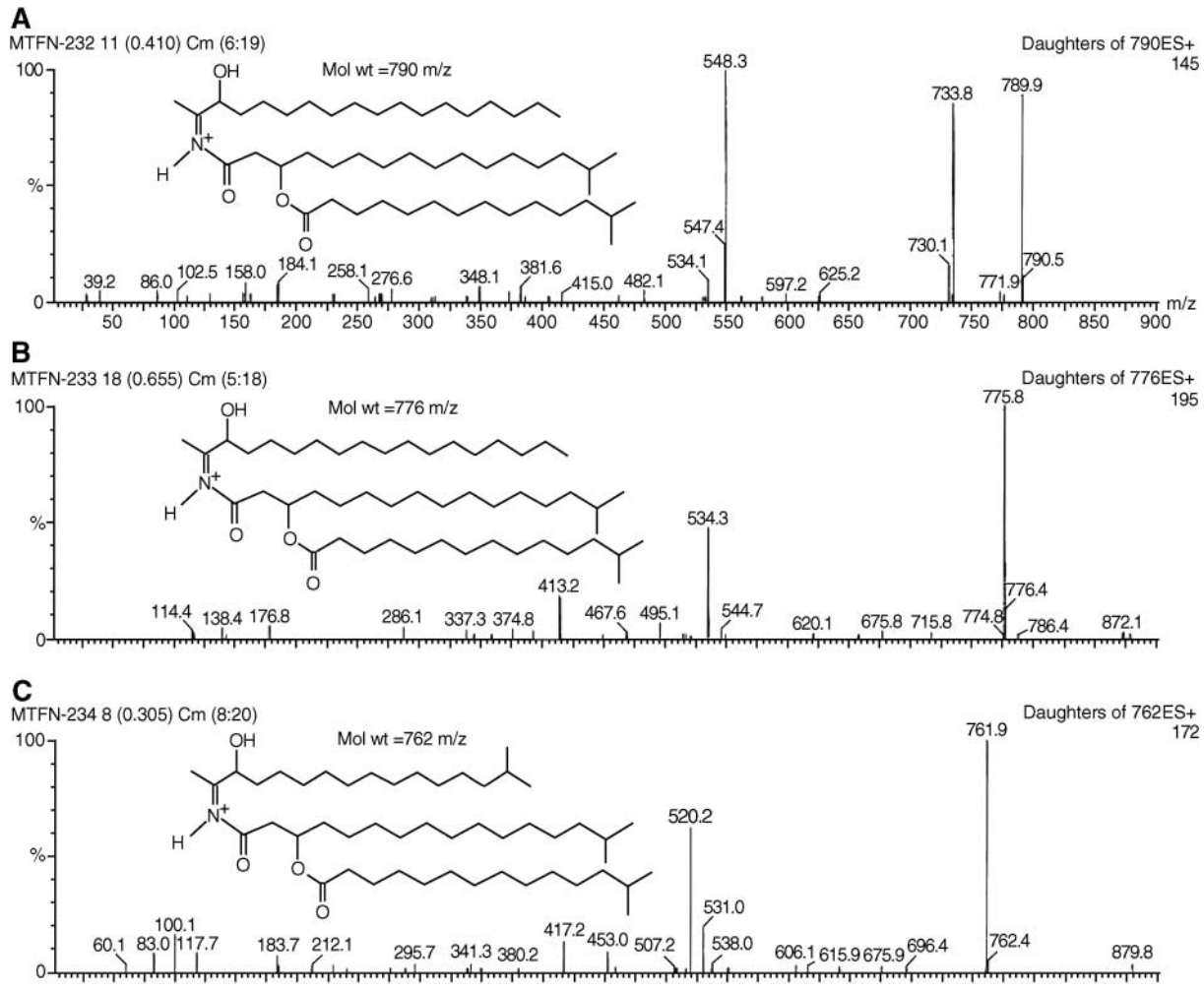

Fig. 4. ESI (+) MS/MS of the 790, 776 and 762 *m/z* parent dihydroceramide ions of *P. gingivalis*. The ESI (+) MS/MS analysis is described in the Materials and Methods section. The chemical structures depicted in frames A, B, and C represent the proposed parent ion structures for the 790, 776, and 762 *m/z* ions, respectively. The structures of 548, 534, and 520 *m/z* daughter ions are shown in Figure 3.

well-separated dihydroceramide lipid classes. The free dihydroceramides recovered in HPLC fractions 7–8 corresponded to the free dihydroceramides of *P. gingivalis* containing 3-OH $C_{17:0}$ in amide linkage to saturated dihydroxy long-chain bases of either 17, 18, or 19 carbons in length (2). Treatment of gingival fibroblasts with fraction 7–8 lipids did not promote IL-1β-mediated prostaglandin secretion, and this ceramide fraction was not further purified. GC-MS analysis of fractions 15–20 and 31–34 suggested dihydroceramide lipid structures termed phosphoglycerol (PG) ceramides and phosphoethanolamine (PEA) ceramides, respectively. Fractions 15–20 were pooled and repurified by HPLC, and peak dihydroceramide lipid recovery was noted in HPLC fraction 20. Fractions 31–34 were repurified by HPLC, and the peak dihydroceramide recovery was noted in HPLC fraction 28.

Positive- and negative-ion ESI-MS analysis of fraction 20 lipids produced the mass spectra shown in **Fig. 2**. The negative-ion spectra (Fig. 2B) revealed three major ions of 960, 946, and 932 *m/z*. Therefore, the masses of the intact lipids are inferred to be greater by 1 amu. Analysis of NMR spectra provided proton and carbon assignments as shown in **Table 1**. The proton and carbon spectra are assigned by number to the dihydroceramide structures proposed (Fig. 2B) (see below). The positive-ion spectra (Fig. 2A) revealed high-mass ions (984, 970, and 956 *m/z*), consistent with sodium adducts of the negative ions shown in the lower frame. The positive-ion mass spectra also demonstrated two additional groups of positive ions (790/791, 776/777, and 762/763 *m/z*, and 548, 534, and 520 *m/z*). Positive-ion MS/MS analysis revealed that the 962, 948, and 934 *m/z* parent ions produce daughter ions of 548, 934, and 920 *m/z*, respectively (**Fig. 3**). The 791, 777, and 763 parent ions also produced daughter ions of 548, 534, and 520 *m/z*, respectively (**Fig. 4**). In all cases, the parent or daughter ions within each group differed in mass by 14 amu increments, suggesting methyl addition to a specific aliphatic chain within the parent lipids. The negative-ion MS/MS spectra revealed 171 and 158 *m/z* daughter ions from the 962, 948, and 934 parent ions (**Fig. 5**). There-

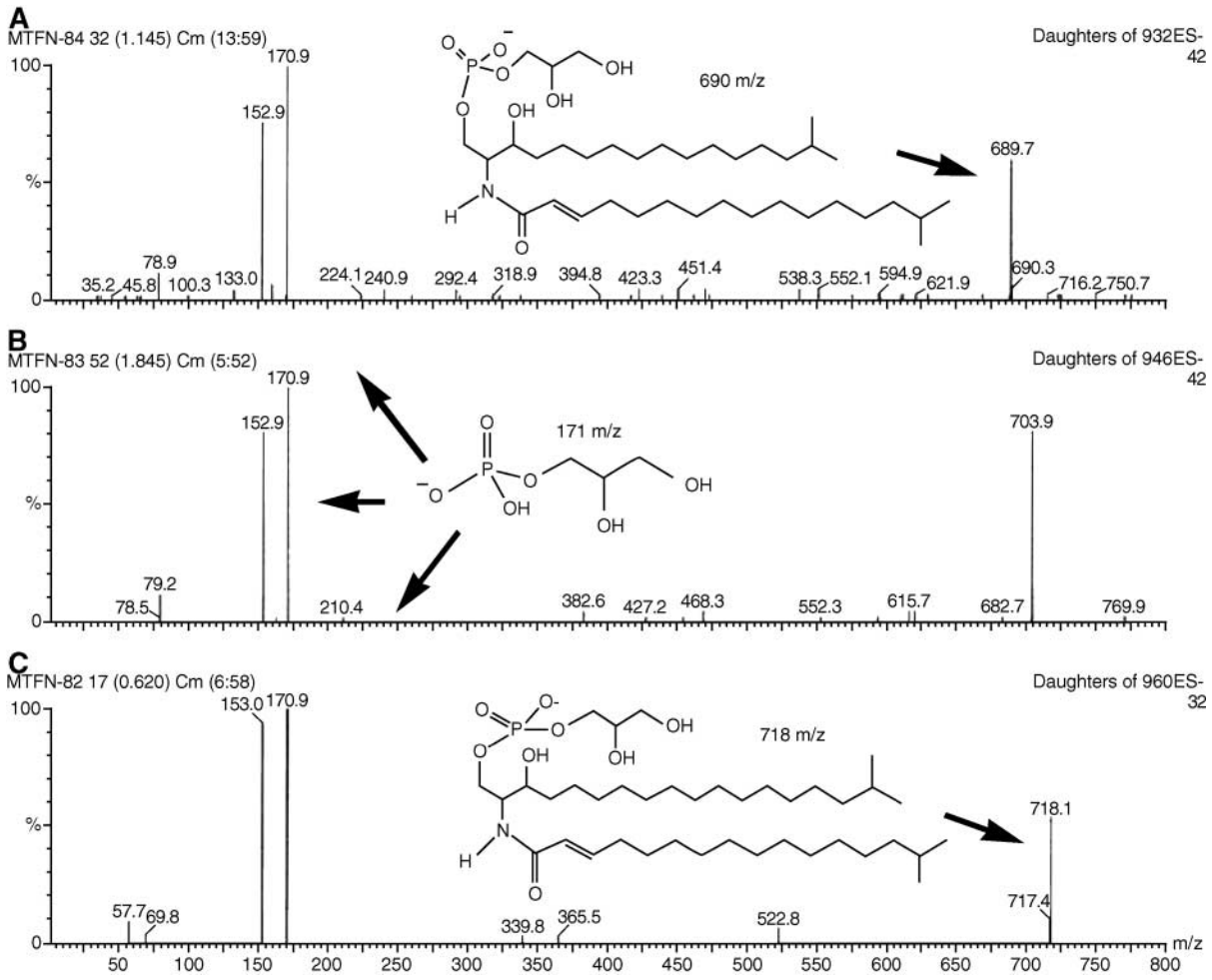

Fig. 5. ESI (−) MS/MS of the 960, 946, and 932 *m/z* parent phosphoceramides of *P. gingivalis*. The ESI (−) MS/MS analysis is described in the Materials and Methods section. A: Proposed phosphoceramide structure for the 690 *m/z* parent ion. B: The structure of the phosphoceramide includes a 1-*O*-phosphoglycerol-substituted octadecanoic long-chain base and an amide-linked 3-OH *iso*$C_{17:0}$ substituent. C: Proposed phosphoceramide structure for the 718 *m/z* parent ion. The 171 *m/z* daughter ions recovered for the three parent negative ions represent the phosphoglycerol head group and the 153 *m/z* daughter ions represent the phosphoglycerol group after dehydration (loss of H_2O).

fore, the 791, 777, and 763 *m/z* ions noted in Fig. 2 represent the loss of a 171 *m/z* ion (phosphoglycerol moiety) from the parent lipid molecules.

NMR analysis of HPLC fraction 20 lipids revealed a proton resonance at 5.22 ppm with HMBC correlations to carbonyl carbons at 170.5 and 173.9 ppm (see Table 1). Combined with other NMR data, these resonances allowed the assignment of the fatty acid substitution on the β hydroxyl of 3-OH-$C_{17:0}$, with methyl branches at the terminal aliphatic chain regions of the fatty acids. TOCSY (long-range ^{1}H-^{1}H COSY) and COSY data related protons of the long-chain dihydroceramide base, and HMQC data were used to assign the ^{13}C data to this backbone. Finally, ^{1}H-^{31}P (gHMBC) and TOCSY data were used to assign the phosphoglycerol attachment to the carbons at 64.2 and 66.4 ppm, as relayed by the protons at 4.20, 3.88, and 3.85 ppm.

Electrospray MS analysis of HPLC fraction 20 lipids dissolved in uniformly labeled deuterated methanol increased positive parent ion masses by 6 amu and increased negative parent ion masses by 4 amu (data not shown). Negative-ion MS/MS with deuterated methanol increased the mass of the 171 daughter ions by 3 amu (data not shown), consistent with a phospoglycerol moiety within these HPLC fraction 20 lipids.

GC-MS analysis further clarified the structures of the fraction 20 lipids. TMS derivatives of fraction 20 lipids revealed the mass spectra shown in **Fig. 6**. The high-mass ions of the three dihydroceramide lipids are recovered as proton adducts of the M-15 ions (nitrogen forms a proton adduct, thus increasing the mass of each dihydroceramide lipid by 1 amu). Loss of the phosphoglycerol moiety due to thermal decomposition in the GC injection block is associated with desaturation of the long-chain base and formation of an imine (see Results, HPLC fraction 28). The HPLC fraction 20 lipids shown in Fig. 6 represent TMS derivatives minus a methyl group (605, 591, and 577 *m/z*) of the daughter ions shown in Figs. 3 and 4 (548, 534, and

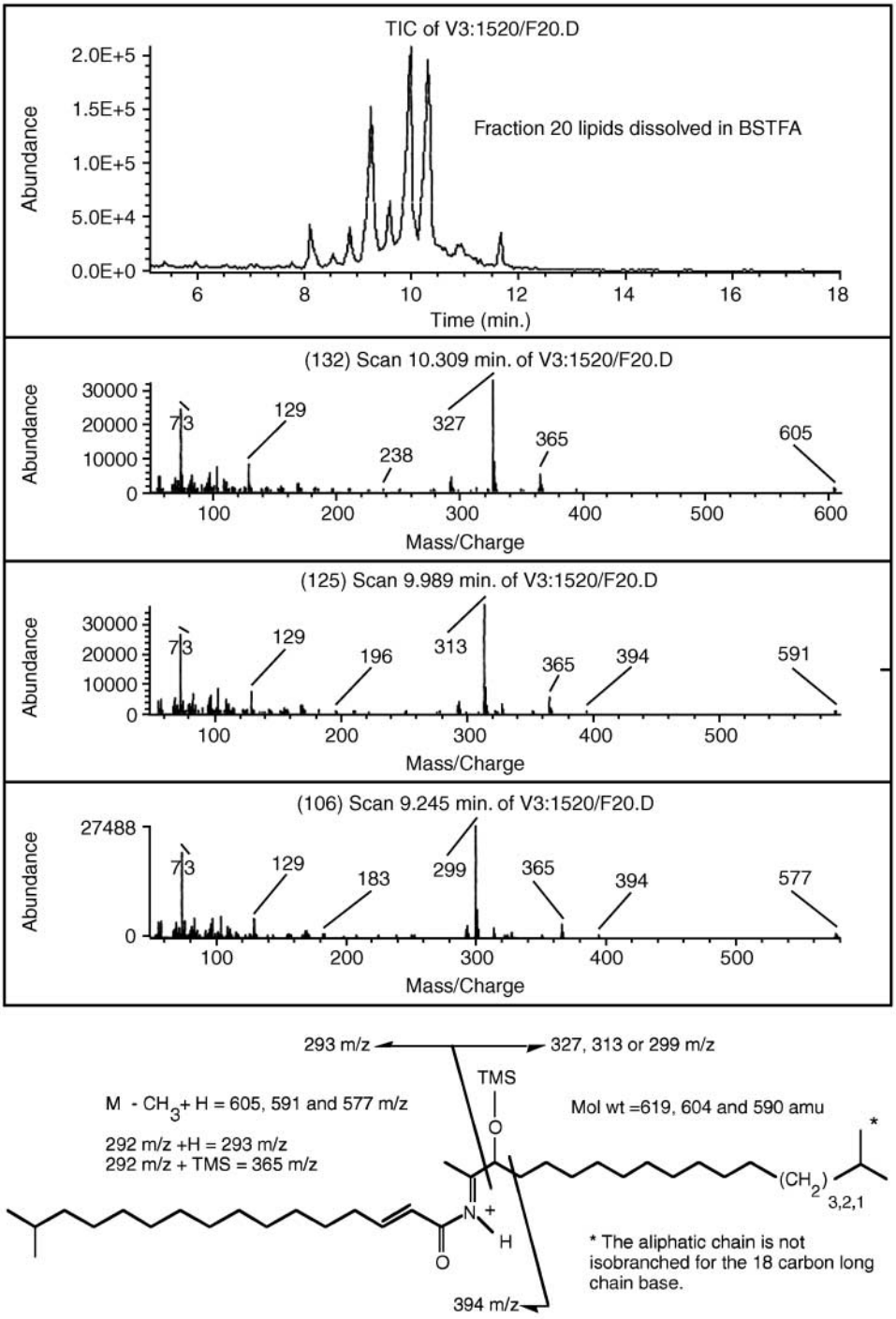

Fig. 6. GC-MS analysis of trimethylsilyl (TMS) derivatives of fraction 20 lipids. GC-MS analysis of fraction 20 dihydroceramides is described in the Materials and Methods section. The upper frame depicts the total ion chromatogram (TIC) of TMS derivatives of fraction 20 lipids. Three major lipid derivatives were recovered, as indicated by retention time (10.309, 9.989, and 9.245 min). The proposed structures of TMS derivatives are shown in the lower frame.

520 *m/z*). Therefore, the lipid derivatives observed by GC-MS (Fig. 6) are consistent with the addition of a single TMS moiety to the smallest daughter ions (548, 534, and 520 *m/z* ions).

Hydrolysis of fraction 20 lipids with sodium methoxide recovered only *iso*$C_{15:0}$ methyl ester, as verified with a synthetic fatty acid standard (data not shown). Treatment of fraction 20 lipids with 4N KOH revealed saturated long-chain bases of 17, 18, and 19 carbons in length and 3-OH *iso*$C_{17:0}$ (data not shown). Based on the retention times of synthetic straight-chain (18 and 20 carbons) and iso-branched long-chain base lipid standards (17 and 19 car-

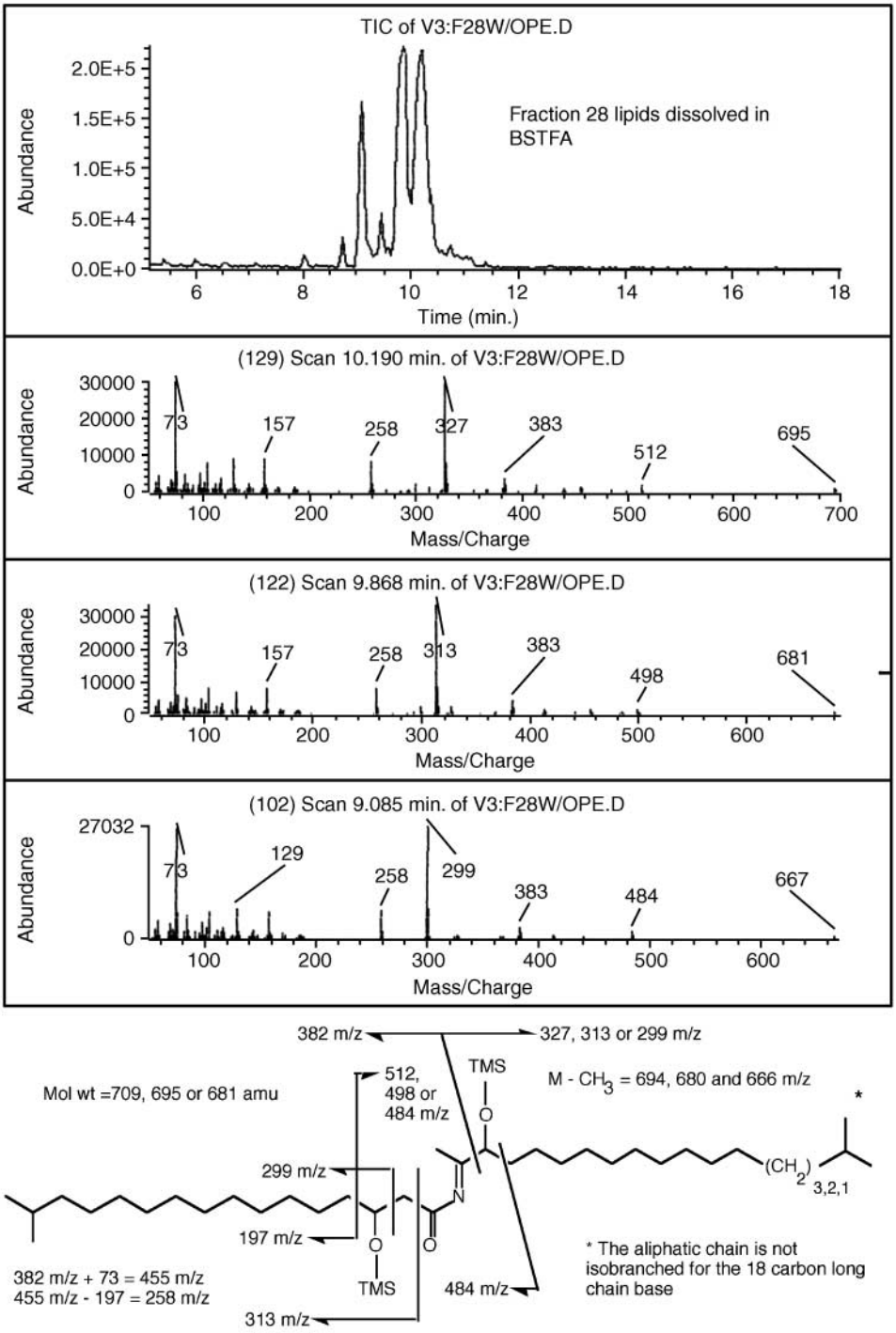

Fig. 7. GC-MS analysis of TMS derivatives of HPLC fraction 28 lipids. Fraction 28 lipids and derivatives were prepared as described in the Materials and Methods section. The upper frame shows the TIC of fraction 28 TMS derivatives. Three major lipid derivatives were recovered, as indicated by retention time (10.229, 9.868, and 9.085 min). The proposed structures of TMS derivatives are shown in the lower frame.

bons), the 17- and 19-carbon long-chain bases of *P. gingivalis* are isobranched saturated long-chain bases, and the 18-carbon long-chain base is a straight long-chain base (data not shown). 3-OH *iso*$C_{17:0}$ was released only with strong alkaline hydrolysis, indicating that this fatty acid is held in amide linkage. The dihydroceramide lipids of fraction 20 therefore consist of 3-OH *iso*$C_{17:0}$ in amide linkage to 17-, 18-, or 19-carbon saturated long-chain bases substituted with a phosphoglycerol moiety linked to the long-chain bases. Reconciliation of the smallest daughter ions of fraction 20 lipids (548, 534, and 520 *m/z* ions) and the position of the esterified *iso*$C_{15:0}$ will be provided in the Discussion section.

The structures of HPLC fraction 20 phosphoglycerol di-

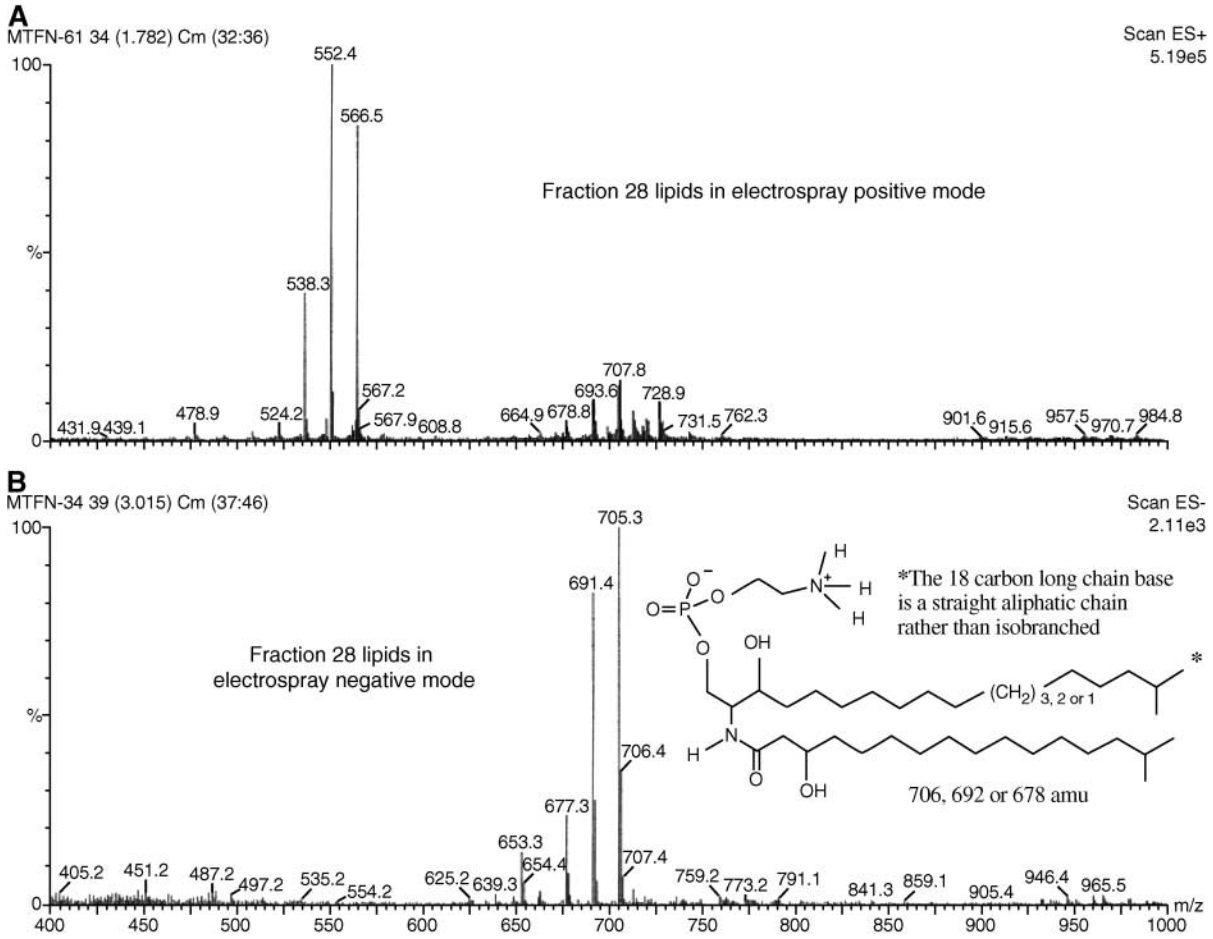

Fig. 8. ESI-MS of HPLC fraction 28 lipids. See the Materials and Methods section for the details of the ESI-MS analyses. A: The ESI (+) mass spectra for fraction 28 lipids. B: The ESI (−) mass spectra and the proposed phosphoceramide structures. Details of the structural reconciliation are reviewed in the Results and Discussion sections.

hydroceramides were further clarified by analysis of HPLC fraction 28 lipids. GC-MS analysis of TMS derivatives of HPLC fraction 28 lipids revealed three major lipid products with associated mass spectra (**Fig. 7**). These lipid derivatives show mass spectra identical to those shown for the previously reported unsaturated ceramides (2). Of note, treatment of fraction 20 lipids with sodium methoxide and GC-MS analysis of the resultant TMS dihydroceramide lipid derivatives demonstrated spectra identical to those depicted in Fig. 7 (data not shown). Therefore, the core lipid structures for dihydroceramides of fraction 20 are identical to the core structures of fraction 28 dihydroceramide lipids. As with fraction 20 lipids, GC-MS of TMS derivatives of fraction 28 lipids at the high injection temperature is associated with thermal decomposition and loss of the phosphorylated head group and desaturation of the proximal end of the long-chain base, resulting in formation of an imine. This was verified by subjecting sphingomyelin and phosphatidylcholine standards to GC-MS under identical conditions. For both lipid standards, the observed mass spectra were consistent with loss of the phosphorylated head group, together with desaturation of either the long-chain base or the glycerol moiety, respectively. Finally, alkaline hydrolysis of fraction 28 lipids released essentially only 3-OH *iso*$C_{17:0}$ (data not shown), indicating that unsaturation does not exist in the fatty acid component of these lipids. It is concluded that the phosphoceramides of HPLC fractions 28 and 20 undergo thermal decomposition in the injection block held at 310°C, and this results in loss of the phosphorylated head group together with formation of a monounsaturated ceramide.

ESI-MS analysis of fraction 28 lipids resulted in positive- and negative-ion spectra, as shown in **Fig. 8**. Figure 8B depicts three negative-ion products differing in mass by 14 amu (705, 691, and 677 *m/z*), whereas Fig. 8A demonstrates the corresponding positive ions (707, 693, and 679 *m/z*), as well as three ions reduced in mass by 141 amu (566, 552, and 538 *m/z*, respectively). Positive-ion MS/MS revealed 566, 552, and 538 *m/z* daughter ions of the 707, 693, and 679 *m/z* parent ions, respectively, indicating loss of a phosphethanolamine head group (data not shown). Negative-ion MS/MS revealed 140 *m/z* daughter ions for the 705, 691, and 677 parent ions (**Fig. 9**). ESI-MS/MS analysis of HPLC fraction 28 lipids dissolved in uniformly labeled deuterated methanol increased positive parent

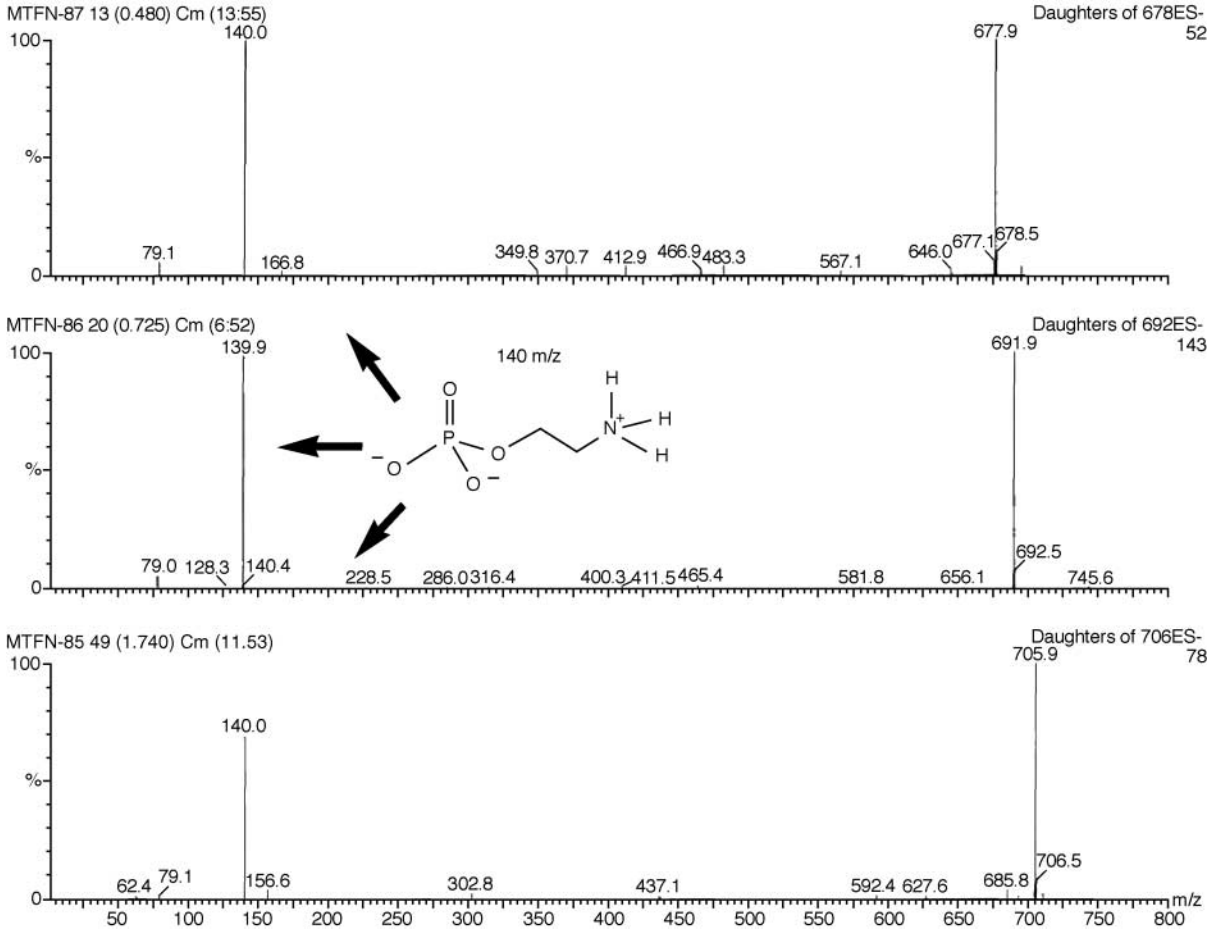

Fig. 9. ESI (−) MS/MS of the 706, 692, and 678 *m/z* parent phosphoceramides of fraction 28 lipids. The ESI (−) MS/MS analysis is described in the Materials and Methods section. The 140 *m/z* daughter ion recovered for the three parent negative ions represents the phosphoethanolamine head group of the three phosphoethanolamine dihydroceramides recovered in fraction 28 lipids.

ion masses by 7 amu and negative parent ion masses by 5 amu (data not shown). Negative-ion ESI-MS/MS using deuterated methanol solvent increased the 140 *m/z* daughter ion masses by 3 amu (data not shown). Deuterium substitution findings are consistent with the number of exchangeable protons expected for the intact dihydroceramides and phosphoethanolamine head group of HPLC fraction 28 phosphoceramides. The phosphoethanolamine location in fraction 28 lipids is reconciled by identifying the position of the unsaturated moiety using GC-MS (Fig. 7). The location of the phosphoglycerol moiety in HPLC fraction 20 lipids is confirmed by applying the same reasoning (see Fig. 6). Therefore, fraction 28 lipids represent three distinct 1-*O*-phosphoethanolamine dihydroceramides containing long-chain bases of 17, 18, or 19 carbons in amide linkage with 3-OH *iso*$C_{17:0}$.

Treatment of gingival fibroblasts with the bacterial lipid fractions demonstrated significant potentiation of IL-1β-mediated PGE_2 secretion from primary cultures of gingival fibroblasts (**Fig. 10**). However, HPLC fraction 20 lipids significantly stimulated PGE_2 release over controls, IL-1β-treated cultures, and cultures treated with HPLC fraction 28 lipids ($P < 0.0001$ by Fisher PLSD and Scheffe F-tests). $PGF_{2\alpha}$ secretion was unaffected by bacterial lipids, and 6-keto $PGF_{1\alpha}$ secretion was modestly increased by the bacterial lipids, but the differences between the treatment groups were not statistically significant. Therefore, the primary effect of bacterial lipids on prostaglandin synthesis was to potentiate PGE_2 secretion over other major prostaglandin species released from IL-1β-stimulated fibroblasts. Of note, bacterial lipids alone did not stimulate prostaglandin secretion, when compared with vehicle controls (data not shown). The total lipid extract of *P. gingivalis* also potentiated prostaglandin secretory responses but to a lesser extent than HPLC fraction 20 lipids. Fibroblast morphology in culture was dramatically affected by fraction 20 lipids and, to a lesser extent, the total lipid extract of *P. gingivalis* (**Fig. 11**). The morphological changes in gingival fibroblasts were noted with or without IL-1β treatment (data not shown).

DISCUSSION

The present study demonstrates that *P. gingivalis* synthesizes phosphoceramides with a core lipid structure consist-

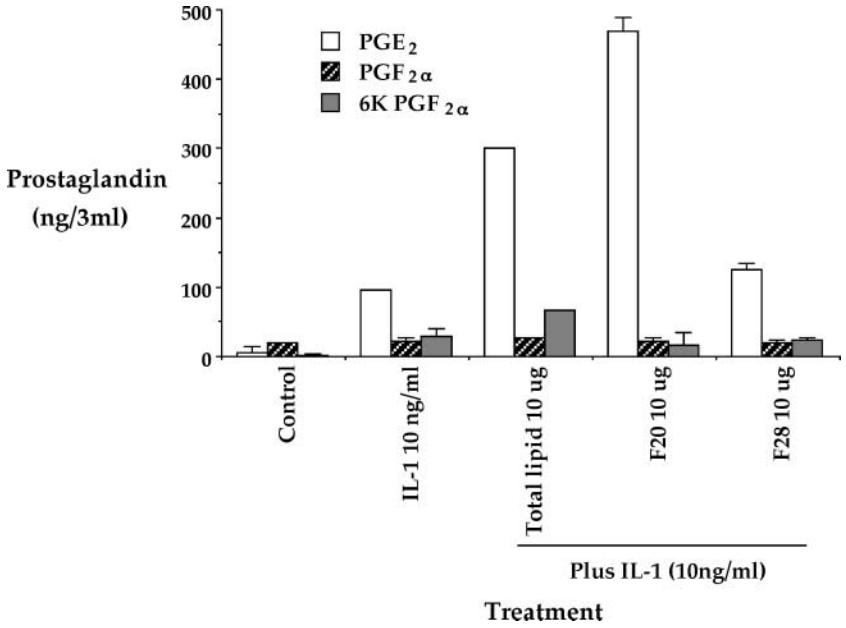

Fig. 10. Prostaglandin secretion from gingival fibroblasts following treatment with lipid fractions derived from *P. gingivalis*. Primary cultures of gingival fibroblasts were obtained from fresh gingival tissue explants as described in the Materials and Methods section. Bacterial lipid extract or specific HPLC fractions were plated into culture dishes at 10 μg/35 mm culture well. Fibroblasts were inoculated into wells and incubated for 2 h, after which the medium was supplemented with human recombinant interleukin-1 (IL-1) (10 ng/ml). Cells were incubated for an additional 24 h, after which medium was harvested and prostaglandin levels determined (see Materials and Methods). Each histogram bar represents the mean for two determinations, and the error bars represent the standard deviation for two determinations. This experiment was conducted twice with similar results for both experiments.

ing of either a 17-, 18-, or 19-carbon long-chain base in amide linkage to 3-OH *iso*$C_{17:0}$. Phosphorylated head groups consist of either phosphoglycerol or phosphoethanolamine, and both head groups are linked to long-chain bases at carbon 1. Of particular note, only the phosphoglycerol dihydroceramide contained *iso*$C_{15:0}$ in ester linkage to the hydroxyl group of 3-OH *iso*$C_{17:0}$. Additional experiments will evaluate whether *P. gingivalis* synthesizes phosphoethanolamine dihydroceramides that contain *iso*$C_{15:0}$ or synthesizes phosphoglycerol dihydroceramides that do not contain *iso*$C_{15:0}$. Although *P. gingivalis* synthesizes a wide variety of fatty acid products, including 3-OH *iso*$C_{15:0}$ and $C_{14:0}$ to $C_{18:0}$ (data not shown), only the fatty acids mentioned above are constituents of the phosphoceramides of *P. gingivalis*. The free dihydroceramides of *P. gingivalis* detected in HPLC fractions 7–8 (data not shown) and described in a previous report (2) likely serve as the substrate molecules for the synthesis of the phosphoceramides described here. Although *P. gingivalis* appears to synthesize phosphoceramides from free dihydroceramide substrates, the details of the synthetic pathways and the specificity of the ceramide substitutions remain for future study.

Both GC-MS and ESI-MS/MS of HPLC fraction 20 lipids produced expected ceramide ions consistent with loss of phosphoglycerol moiety (Figs. 3, 4, 6). However, both analytical methods produce lower-mass ions, consistent with McLafferty rearrangements (14), resulting in loss of esterified *iso*$C_{15:0}$ from the ceramides. McLafferty rearrangements explain the generation of 548, 534, and 520 ions under positive-ion ESI-MS/MS analysis, as well as the formation of the 605, 591, and 577 ions observed with GC-MS analysis of fraction 20 lipids. McLafferty rearrangements produce a monounsaturation of 3-OH *iso*$C_{17:0}$, with loss of the β-position oxygen. An earlier report concluded that the unsaturated ceramides are synthesized by *P. gingivalis* because α-β unsaturated $C_{17:0}$ is recovered in alkaline hydrolyzates of *P. gingivalis* lipids. However, monounsaturated $C_{17:0}$ is not recovered in HPLC fraction 20 lipids (data not shown) and therefore cannot be a constituent of this ceramide fraction. Therefore, the McLafferty rearrangement of fraction 20 lipids that occurs under both GC-MS and ESI-MS/MS conditions indicates that esterified *iso*$C_{15:0}$ exists as a 3-O substitution on 3-OH *iso*$C_{17:0}$. Finally, transesterification of fraction 20 lipids with sodium methoxide eliminates *iso*$C_{15:0}$ from the ceramides and allows 3-O-TMS substitution of 3-OH *iso*$C_{17:0}$ in the fraction 20 dihydroceramides, thus producing mass spectra identical to those observed for fraction 28 phosphoceramides (Fig. 7).

The phosphoceramide lipids presented in this report are consistent with phosphoglycerol and phosphoethanolamine ceramides previously described by White and Tucker for the species *Bacteroides melaninogenicus* (15). Like *B. melaninogenicus*, *P. gingivalis* phosphoceramides also contain isobranched 17- and 19-carbon long-chain bases and a

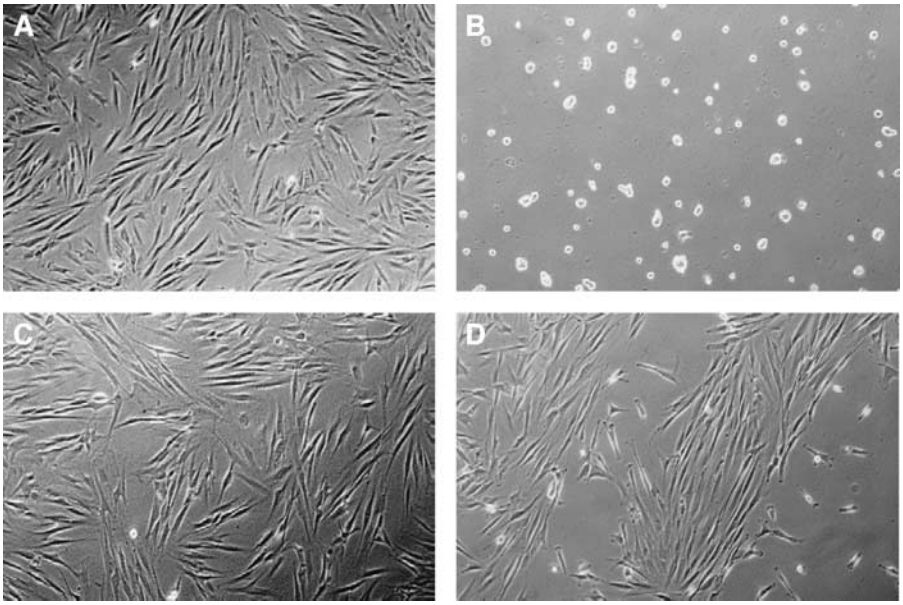

Fig. 11. Effects of *P. gingivalis* lipids on gingival fibroblast morphology in vitro. Gingival fibroblasts treated with the *P. gingivalis* lipid preparations under the conditions described in Fig. 10 were photographed at the end of the 24 h treatment period. Control cells (A) appear essentially the same as cells treated with IL-1β (results not shown). Fibroblasts exposed to F20 (B), F28 (C), or total lipid extract (D) followed by IL-1β appear as cells treated with these bacterial lipid preparations without IL-1β (results not shown).

saturated straight-chain 18-carbon long-chain base (16). However, we did not recover fatty acids other than amide-linked 3-OH *iso*$C_{17:0}$ and ester-linked *iso*$C_{15:0}$ in the biologically active phosphoceramides of *P. gingivalis*, in contrast to *B. melaninogenicus* phosphoceramides that contain a variety of saturated and monounsaturated fatty acids (15). Therefore, the phosphoceramides of *P. gingivalis* appear to have specific fatty acid substitutions when compared with *B. melaninogenicus* phosphoceramides.

Other bacterial species are known to synthesize ceramide-like lipids that share structural characteristics with *P. gingivalis* ceramides. *Sphingobacterium* species are reported to synthesize phosphoethanolamine ceramides containing a 15-methyl hexadecanoic long-chain base in amide linkage to either *iso*$C_{15:0}$ or 2-OH *iso*$C_{15:0}$ (4, 17). Neither phosphoglycerol ceramides nor ester-linked fatty acid were reported for *Sphingobacterium* phosphoceramides (4, 17). These bacterial sphingolipids were recently shown to promote apoptosis in several cell types (4). Because of the structural similarities between *P. gingivalis* phosphoceramides and *Sphingobacterium* sp. phosphoceramides, it is expected that *P. gingivalis* phosphoceramides will induce apoptosis as well. More importantly, the phosphoglycerol ceramides of *P. gingivalis* demonstrate considerably greater biological activity than do the phosphoethanolamine ceramides. Other bacteria produce lipids that are more distantly related to the phosphoceramides of *P. gingivalis*. These include *Flavobacterium meningosepticum*, which synthesizes a flavolipin consisting of an amide-linked isobranched fatty acid linked to a serine-glycine isobranched aliphatic amino alcohol (18). Finally, *Capnocytophaga* species synthesize sulfonolipids (capnines) that contain sulfonate isobranched long-chain bases (19, 20). Despite this evidence, the phosphoceramides of *P. gingivalis* characterized in this report suggest novel lipids that are distinct from those produced by other organisms.

The free dihydroceramides of *P. gingivalis* (2) recovered in fractions 7–8 are without the capacity to potentiate prostaglandin secretion from gingival fibroblasts, a surprising result, given the reported capacity of free ceramides to promote prostaglandin secretion from fibroblasts (21, 22) and other cells (23). However, those HPLC fractions shown to contain the phosphoglycerol dihydroceramides markedly promoted PGE_2 secretion from IL-1β-treated fibroblasts, indicating that these phosphoceramides account for at least a major portion of the biological activity observed in the total lipid extract of *P. gingivalis*. The biological relevance of the phosphoglycerol dihydroceramides relates to the capacity of these lipids to promote inflammatory processes associated with periodontal diseases and perhaps other systemic inflammatory diseases associated with bacterial lipid accumulation. It is suspected that the phosphoglycerol dihydroceramides of *P. gingivalis* produce their biological effects through a recognized pattern recognition system (Toll receptor) or interact with an as-yet uncharacterized pattern recognition system in human cells. Whether the highly lipophilic phosphoglycerol dihydroceramides affect cell activity through interaction with a cell surface receptor or an intramembranous protein constituent remains to be established. Penetration of bacterial lipid into inflamed periodontal tissues without coincident bacterial invasion (24) would be expected to intensify the inflammatory reaction such that bone and connective tissue destruction could be fa-

vored through locally increased synthesis of PGE_2 (25, 26). GC-MS has shown that lipid extracts from periodontally diseased teeth and diseased periodontal soft tissues are contaminated ceramide structures, consistent with the phosphoglycerol ceramide products shown in Fig. 6 (data not shown).

Therefore, the results of this study demonstrate that a major periodontal pathogen, *P. gingivalis*, synthesizes a group of unusual, complex lipids, specifically phosphoglycerol ceramides, that account in part for the ability of *P. gingivalis* lipid extract to potentiate IL-1β-mediated prostaglandin secretion from fibroblasts. The marked potentiation of prostaglandin synthesis is not observed with the structurally similar phosphoethanolamine dihydroceramide class described herein, indicating that the specific structural characteristics of the phosphoglycerol dihydroceramides account for the marked potentiation of IL-1β-mediated prostaglandin secretion. In addition to potentiation of prostaglandin secretion from gingival fibroblasts, the phosphoglycerol dihydroceramides of *P. gingivalis* dramatically alter fibroblast morphology in culture (Fig. 11) and alter gene expression for a substantial number of proinflammatory and signal transduction genes, as measured by Affymetrix focused gene array (data not shown). Furthermore, at least one additional lipid class of *P. gingivalis* promotes similar cell activation events. Space limitations prevent inclusion of these new findings. Understanding the basis for cell activation following exposure to phosphoglycerol dihydroceramide lipids or synthetic chemical analogs will be of considerable importance in understanding diseases associated with accumulation of these agents in tissues.

The authors would like to thank Ms. Jody Barry for her assistance in the microbiological preparation of *P. gingivalis*. The authors would also like to thank Mr. Marvin Thompson for his assistance in the electrospray mass spectral analysis of the lipid compounds. The authors also thank Dr. Clarence Trummel for providing funds to cover publication costs. This work was supported in part by a grant from the Patterson Trust Foundation.

REFERENCES

1. Holt, S. C., L. Kesavalu, S. Walker, and C. A. Genco. 1999. Virulence factors of Porphyromonas gingivalis. *Periodontol 2000.* **20:** 168–238.
2. Nichols, F. C. 1998. Novel ceramides recovered from *Porphyromonas gingivalis*: relationship to adult periodontitis. *J. Lipid Res.* **39:** 2360–2372.
3. Nichols, F., H. Levinbook, M. Shnaydman, and J. Goldschmidt. 2001. Prostaglandin E_2 secretion from gingival fibroblasts treated with interleukin-1β: effects of lipid extracts from *P. gingivalis* or calculus. *J. Periodontal Res.* **36:** 142–152.
4. Minamino, M., I. Sakaguchi, T. Naka, N. Ikeda, Y. Kato, I. Tomiyasu, I. Yano, and K. Kobayashi. 2003. Bacterial ceramides and sphingophospholipids induce apoptosis of human leukaemic cells. *Microbiol.* **149:** 2071–2081.
5. Miyagawa, E., R. Azuma, T. Suto, and I. Yano. 1979. Occurrence of free ceramides in *Bacteroides fragilis* NCTC 9343. *J. Biochem. (Tokyo).* **86:** 311–320.
6. Bligh, E. G., and W. J. Dyer. 1959. A rapid method of total lipid extraction and purification. *Can. J. Med. Sci.* **37:** 911–917.
7. Garbus, J., H. F. DeLuca, M. E. Loomas, and F. M. Strong. 1968. Rapid incorporation of phosphate into mitochondrial lipids. *J. Biol. Chem.* **238:** 59–63.
8. Geurts Van Kessel, W. S. M., W. M. A. Hax, R. A. Demel, and J. De Gier. 1977. High performance liquid chromatographic separation and direct ultraviolet detection of phospholipids. *Biochim. Biophys. Acta.* **486:** 524–530.
9. Richards, D., and R. B. Rutherford. 1988. The effects of interleukin-1 on collagenolytic activity and prostaglandin E secretion by human periodontal ligament and gingival fibroblasts. *Arch. Oral Biol.* **33:** 237–243.
10. Luderer, J. R., D. L. Riley, and L. M. Demers. 1983. Rapid extraction of arachidonic acid metabolites utilizing octadecyl reversed-phase columns. *J. Chromatogr.* **273:** 402–409.
11. Waddell, K. A., I. A. Blair, and J. Wellby. 1983. Combined capillary column gas chromatography negative ion chemical ionization mass spectrometry of prostanoids. *Biomed. Mass Spectrom.* **10:** 83–88.
12. Nimkar, S., D. Menaldino, M. A.H. and D. Liotta. 1988. A stereoselective synthesis of sphingosine, a protein kinase C inhibitor. *Tetrahedron Lett.* **29:** 3037–3040.
13. Takikawa, H., D. Nozawa, A. Kayo, S. Muto, and K. Mori. 1999. Synthesis of sphingosine relatives. Part 22. Synthesis of sulfobacin A, B and flavocristamide A, new sulfonolipids isolated from Chryseobacterium sp. *J. Chem. Soc. Perkin Trans.* **1:** 2467–2477.
14. McLafferty, F. W., and F. Turecek. 1993. Interpretation of Mass Spectra. University Science Books, Sausalito, CA.
15. White, D. C., and A. N. Tucker. 1970. Ceramide phosphorylglycerol phosphate: a new sphingolipid found in bacteria. *Lipids.* **5:** 56–62.
16. White, D. C., A. N. Tucker, and C. C. Sweeley. 1969. Characterization of the *iso*-branched sphinganines from the ceramide phospholipids of *Bacteroides melaninogenicus*. *Biochim. Biophys. Acta.* **187:** 527–532.
17. Naka, T., N. Fujiwara, I. Yano, S. Maeda, M. Doe, M. Minamino, N. Ikeda, Y. Kato, K. Watabe, Y. Kumazawa, I. Tomiyasu, and K. Kobayashi. 2003. Bacterial ceramides and sphingophospholipids induce apoptosis of human leukaemic cells. *Biochim. Biophys. Acta.* **149:** 2071–2081.
18. Kawai, Y., I. Yano, and K. Kaneda. 1988. Various kinds of lipoamino acids including a novel serine-containing lipid in an opportunistic pathogen Flavobacterium. Their structures and biological activities on erythrocytes. *Eur. J. Biochem.* **171:** 73–80.
19. Godchaux III, W., and E. R. Leadbetter. 1984. Sulfonolipids of gliding bacteria. Structure of the N-acylaminosulfonates. *J. Biol. Chem.* **259:** 2982–2990.
20. Godchaux III, W., and E. R. Leadbetter. 2003. Structural analysis of sphingophospholipids derived from Sphingobacterium spiritivorum, the type species of genus Sphingobacterium. *J. Bacteriol.* **1635:** 83–92.
21. Ballou, L. R., C. P. Chao, M. A. Holness, S. C. Barker, and R. Raghow. 1992. Interleukin-1-mediated PGE_2 production and sphingomyelin metabolism. Evidence for the regulation of cyclooxygenase gene expression by sphingosine and ceramide. *J. Biol. Chem.* **267:** 20044–20050.
22. Kirtikara, K., S. J. Laulederkind, R. Raghow, T. Kanekura, and L. R. Ballou. 1998. An accessory role for ceramide in interleukin-1beta induced prostaglandin synthesis. *Mol. Cell. Biochem.* **181:** 41–48.
23. Pfau, J. C., E. B. Walker, and G. L. Card. 1998. A comparison of the effects of lipopolysaccharide and ceramide on arachidonic acid metabolism in THP-1 monocytic cells. *Cell. Immunol.* **186:** 147–153.
24. Nichols, F. C. 1994. Distribution of 3-hydroxy iC17:0 in subgingival plaque and gingival tissue samples: relationship to adult periodontitis. *Infect. Immun.* **62:** 3753–3760.
25. Klein, D. C., and L. G. Raiz. 1970. Prostaglandins: stimulation of bone resorption in tissue culture. *Endocrinology.* **86:** 1436–1440.
26. Goodson, J. M., F. E. Dewhirst, and A. Brunetti. 1974. Prostaglandin E_2 levels and human periodontal disease. *Prostaglandins.* **6:** 81–85.